

Coulomb explosion of N₂ using intense 10- and 40-fs laser pulses

E. Baldit, S. Saugout, and C. Cornaggia

Direction des Sciences de la Matière, Service des Photons, Atomes et Molécules, CEA Saclay, Bâtiment 522, F-91 191 Gif-sur-Yvette, France

(Received 25 November 2004; published 23 February 2005)

Intense laser pulse duration effects in the Coulomb explosion of the N₂ molecule are studied using 10- and 40-fs laser pulses in the 10¹⁴–10¹⁶ W cm⁻² intensity range. At 10 fs, no significant molecular stretching is observed during multi-ionization events up to the N²⁺+N²⁺ fragmentation channel. Kinetic energy releases are larger and fragmentation yields are lower at 10 fs than at 40 fs due to the 1/*R* scaling of the molecular multi-ionization thresholds. These results open the way to Coulomb explosion imaging of neutral molecules using intense sub-10-fs laser pulses.

DOI: 10.1103/PhysRevA.71.021403

PACS number(s): 33.80.Rv, 33.80.Eh, 42.50.Vk

Coulomb explosion imaging is used in beam-foil experiments. Very short interaction times of the order of 0.1 fs within the foil allow us to get the instantaneous positions of atoms in the molecule [1]. In the late 1980s and early 1990s, Coulomb explosion was demonstrated using intense picosecond and femtosecond laser pulses [2,3]. Since then, many studies have been devoted to molecules and clusters in strong laser fields [4]. Laser pulse durations of several tens of femtoseconds remain long in comparison with the vibrational periods of molecules. In consequence, the interpretation of the experimental data demands us to take into account the nuclear coordinates evolution during the interaction time [5].

In the same time, intense laser pulses as short as 20 fs became available at the TeraWatt level due to the concept of chirped-pulse amplification associated with the large bandwidth of the Ti:sapphire gain medium [6,7]. The 20-fs pulse duration lower limit is set by gain bandwidth narrowing in the preamplification stage. The generation of 5-fs laser pulses at a 100-GW power level and 1-kHz repetition rate was made possible using two techniques that appeared in the 1990s [8]. The first one relies on pulse spectral broadening, which is achieved by self-phase modulation in a hollow fiber filled with a noble gas [9]. The hollow fiber behaves as a single-mode waveguide where the propagation of intense pulses produces an efficient third-order nonlinear polarization in the atomic medium. The spatially uniform broadened pulses in the frequency domain are then recompressed in the temporal domain down to the Fourier limit using chirped-mirrors technology [10].

In principle, these new developments will open the way to laser-induced Coulomb explosion of molecules without any noticeable nuclear coordinates change during the interaction time. The molecular multi-ionization thresholds scale as 1/*R* where *R* is the internuclear distance. In consequence, excitation and explosion at the molecular equilibrium distance are expected to produce more energetic fragments than in the case where a noticeable stretching occurs before the ionization events. In addition, the corresponding energies deposited in the molecule are higher because of the 1/*R* dependence and the resulting fragmentation yields are expected to be weaker using similar laser intensities.

This paper is aimed at presenting results on the Coulomb explosion induced by intense 10-fs pulses and comparing

them with previous results recorded with 40-fs pulses using comparable laser intensities. The experimental results support the above simple statements about pulse duration effects on molecular Coulomb explosion. In particular, we show that multi-ionization and Coulomb explosion occur at the equilibrium internuclear distance up to the N²⁺+N²⁺ dissociation channel for N₂ using 10-fs laser pulses. Similar results were recorded for the O₂ molecule and will be presented elsewhere.

The main laser system is a 1-kHz Ti:sapphire laser producing 600-μJ, 40-fs laser pulses with a wavelength spectrum centered at 800 nm. The pulse compression setup is designed following the techniques of Nisoli *et al.* [9] and Sartania *et al.* [8]. The laser spectrum is broadened in a 700-mm-long hollow fiber with a 250-μm inner diameter. The nonlinear Kerr effect takes place in argon at a pressure of 700 mbar. After recollimation by an *f*=1 m concave silver mirror, pulses are recompressed using several reflexions on broadband chirped mirrors. The spectrum and pulse duration are measured using, respectively, a commercial spectrometer and a homemade interferometric autocorrelator. Figure 1 presents a spectrum and an autocorrelation of 10-fs pulses. In Fig. 1(a) the spectrum exhibits a three-peak structure over around 200 nm due to self-phase modulation in argon gas. The Fourier transform of the corresponding electric field is introduced in the calculation of the interferometric autocorrelation assuming a given spectral phase. The comparison between the measured and calculated signals is presented in Fig. 1(b). The good agreement shows that the chirped-mirrors compression stage works well. The remaining disagreement comes from the cubic and quartic residual phases that cannot be compensated with our setup. From these measurements and calculations, the pulse duration is found to be 10 fs at full width half maximum in intensity.

Molecular ions and dications, as well as multicharged fragments, are detected using a 1150-mm-long time-of-flight spectrometer based on the Wiley-McLaren configuration [11]. Fragmentation channels and the associated kinetic energy release spectra are determined using the covariance mapping of Frasinski *et al.* [12].

Laser-induced double ionization of N₂ and the resulting N⁺+N⁺ dissociation pattern was investigated in our laboratory using 40-fs laser pulses in the 10¹⁴–10¹⁵ W cm⁻² laser

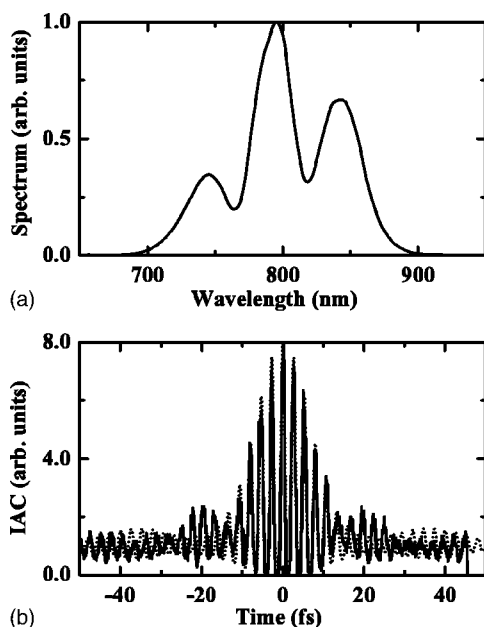


FIG. 1. Ultrashort 10-fs laser pulse. (a) Wavelength spectrum, (b) interferometric autocorrelation (IAC), where the experimental and calculated signals are given, respectively, by the full and dotted curves. The IAC curve is calculated using the Fourier transform of the frequency domain electric field and assuming a constant spectral phase.

intensity range [13,14]. Excitation at the neutral molecule equilibrium internuclear distance and subsequent population of several electronic states of N_2^{2+} were found to be responsible for the metastable N_2^{2+} ion and the $N^+ + N^+$ fragmentation channel simultaneous detections. This conclusion is supported by the fact that the singly charged N_2^+ precursor ion or the neutral molecule in the case of nonsequential double ionization are highly stable. Therefore no large molecular stretchings are expected before double ionization events. This statement is no more valid for fragmentation involving higher molecular charge states such as the $N^{2+} + N^{2+}$ fragmentation channel. In that case, the precursor molecular ion is N_2^{3+} for a single ionization. This molecular ion does not support any quasibound state because Coulomb repulsion is the dominant force even at short internuclear distance [15]. In consequence, depending on the pulse duration, the N_2^{3+} ion has time to stretch out before the ionization event leading to N_2^{4+} and the $N^{2+} + N^{2+}$ fragmentation channel. Therefore, the $N^+ + N^+$ and $N^{2+} + N^{2+}$ kinetic energy release spectra are expected to exhibit different pulse duration dependences.

Figure 2 represents the spectra of N^+ ions from the $N^+ + N^+$ channel at 40 and 10 fs for three different laser intensities. Similar spectra are recorded for both pulse durations. The detected structures in Fig. 2 come from different molecular states of the N_2^{2+} dication and do not depend on the laser intensity. For instance, the electronic states associated with the N^+ peaks at around 4 and 5 eV might, respectively, be the $^1\Delta_g$ and $^1\Pi_g$ states [16]. Other states are equally good candidates because of the very high density of states in this spectral region [17].

The N_2^{4+} molecular ion does not exhibit any bound or quasibound electronic state [18]. In consequence, the elec-

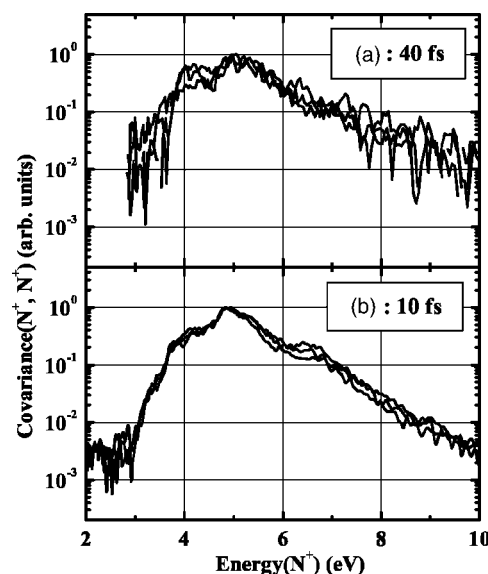


FIG. 2. Normalized covariance energy spectra of N^+ ions from the $N^+ + N^+$ fragmentation channel of N_2 recorded at three peak laser intensities $4 \times 10^{14} \text{ W cm}^{-2}$, $8 \times 10^{14} \text{ W cm}^{-2}$, $2 \times 10^{15} \text{ W cm}^{-2}$, and with different pulse durations (a) 40 fs and (b) 10 fs.

tronic energy increases as the internuclear distance decreases. Figure 3 represents the N^{2+} kinetic energy spectra recorded at 40 and 10 fs using the same peak laser intensity $2 \times 10^{15} \text{ W cm}^{-2}$. Structures labeled A, B, C, and D come from different fragmentation channels involving the N^{2+} ion

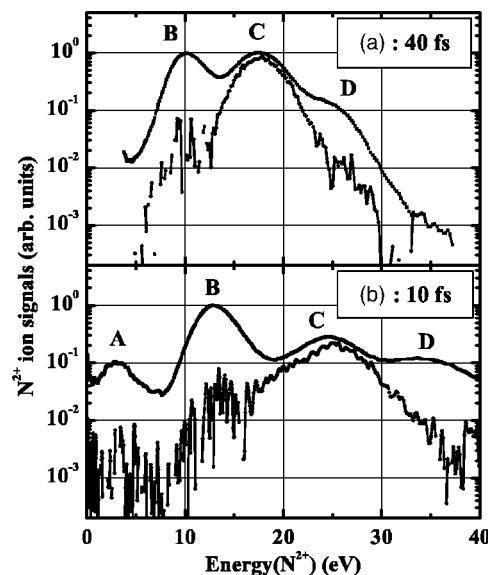


FIG. 3. Kinetic energy spectra of N^{2+} ions from N_2 recorded at $2 \times 10^{15} \text{ W cm}^{-2}$ at (a) 40 fs, and at (b) 10 fs pulse durations. In each case (a) and (b), the upper curves represent spectra of all the detected N^{2+} ions. The labels A, B, C, and D in panels (a) and (b) represent, respectively, the (A) $N^{2+} + N$, (B) $N^{2+} + N^+$, (C) $N^{2+} + N^{2+}$, and (D) $N^{2+} + N^{3+}$ fragmentation channels. These channels are determined using covariance mapping. For instance, the lower curves in (a) and (b) represent the (N^{2+}, N^{2+}) covariance spectra that identify the $N^{2+} + N^{2+}$ fragmentation channel without any ambiguity.

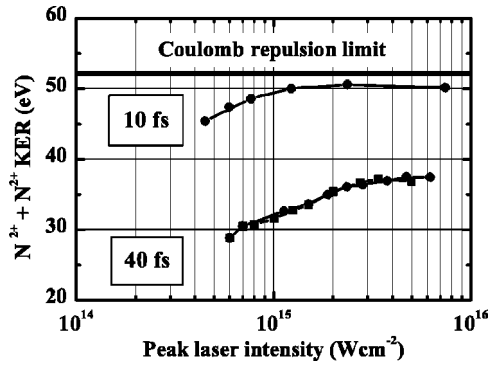


FIG. 4. Kinetic energy releases (KER) of the N²⁺+N²⁺ fragmentation channel at (a) 10 and (b) 40 fs as a function of the peak laser intensity. These energies are the energies of the maxima of the corresponding kinetic energy release spectra. The Coulomb repulsion energy is the electrostatic repulsion energy calculated at $R_e(\text{N}_2)=1.098 \text{ \AA}$.

as it is reported in the caption. The N²⁺+N²⁺ fragmentation channel labeled C is identified by the covariance spectra represented by the lower curves. The first striking observation is the shift towards higher energies when the pulse duration is reduced to 10 fs. This shift simply means that molecular explosion occurs at shorter internuclear distances. In addition, the branching ratio of the N²⁺+N²⁺ channel is weaker at 10 fs than at 40 fs in comparison with the N²⁺+N⁺ channel as it can be seen from the heights of the B and C structures. This result is consistent with higher kinetic energy releases at 10 fs. Indeed, at shorter internuclear distances, the N₂⁴⁺ threshold is higher and in consequence, the corresponding ion yield is weaker than the ion yield obtained at larger internuclear distances.

In Fig. 4, the N²⁺+N²⁺ kinetic energy releases at the ion spectra maxima are summarized as a function of the peak laser intensity for 10 and 40 fs pulses. The energies increase as the laser intensity is increased and in the case of the 10-fs pulses, the kinetic energy release is very close to the Coulomb repulsion energy at high laser intensities. In consequence, the N²⁺+N²⁺ Coulomb explosion takes place at internuclear distances close to the neutral molecule equilibrium distance. The pulse duration and laser intensity dependences in Fig. 4 are explained by the simple following model. Let us take the laser intensity as $I(t)=I_0\exp[-(t/\tau)^2]$ where τ is the pulse duration divided by $2\sqrt{\ln 2}$ and I_0 is the peak laser intensity. Let us assume a sequential ionization scheme leading to the N₂⁴⁺ ion and subsequent instantaneous N²⁺+N²⁺ Coulomb explosion, where the N₂³⁺ precursor ion is created at time t_1 and laser intensity I_1 . Then, the single ionization of this ion at time t_2 and intensity $I_2>I_1$ leads to the observed N²⁺+N²⁺ fragmentation channel. Ionization events are assumed to occur during the pulse rising edge, i.e., at $t_1<t_2<0$. The time delay t_2-t_1 between both ionization events given by

$$t_{21} = t_2 - t_1 = \tau \left\{ \sqrt{\ln(I_0/I_1)} - \sqrt{\ln(I_0/I_2)} \right\} \quad (1)$$

is proportional to the pulse duration. In consequence, long pulses allow more time for molecular stretching due to the

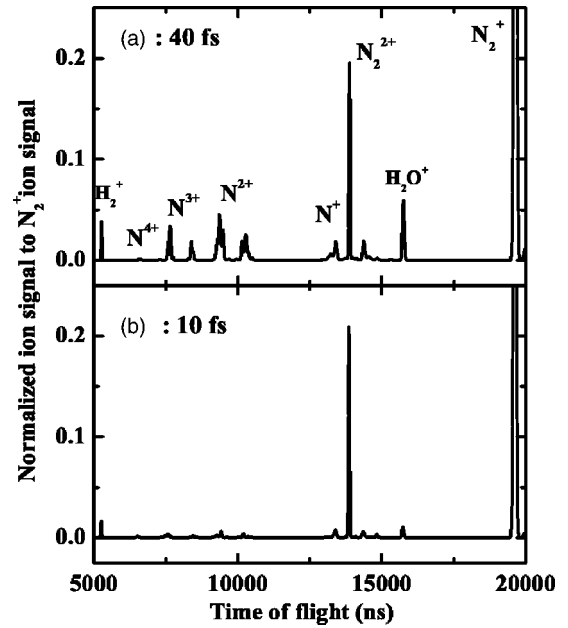


FIG. 5. Time-of-flight spectra of N₂ recorded with different pulse durations and comparable peak laser intensities. (a) 40 fs and $5 \times 10^{15} \text{ W cm}^{-2}$, (b) 10 fs and $7.4 \times 10^{15} \text{ W cm}^{-2}$. The spectra are normalized to the maximum of the N₂⁺ peak. Double-peak structures of ionic fragments come from forward- and backward-emitted ions with respect to the ion detector position.

N₂³⁺ dissociation. The final larger internuclear distance explains the lower kinetic energy releases of the N²⁺+N²⁺ channel in Fig. 4. The peak laser intensity dependences of these energies is explained by the derivative $d(t_2-t_1)/dI_0$, which is a negative number proportional to the pulse duration

$$\frac{d(t_2-t_1)}{dI_0} = -\frac{\tau}{2I_0} \frac{\sqrt{\ln(I_0/I_1)} - \sqrt{\ln(I_0/I_2)}}{\sqrt{\ln(I_0/I_1)}\sqrt{\ln(I_0/I_2)}}. \quad (2)$$

As the laser intensity is increased, less time is left in the pulse rising edge for molecular stretching of the N₂³⁺ ion and in consequence the N²⁺+N²⁺ energies are larger, as in Fig. 4.

Finally, fragmentation yields coming from molecular multiple ionization are expected to be smaller at 10 fs because of higher ionization potentials at short internuclear distances. This point is confirmed by Fig. 5, which represents two time-of-flight spectra recorded using 40- and 10-fs laser pulses and comparable peak laser intensities. Both spectra are normalized to the N₂⁺ peak in order to compare the fragmentation ratios. Although the 10-fs pulse intensity is chosen to be higher than the 40-fs pulse, Fig. 5 shows clearly that fragmentation is much less pronounced using the 10-fs laser pulse. The N₂²⁺ peak comes from detected metastable dications and exhibits the same height in both spectra. It simply comes from saturation of this channel at high laser intensities. In this case, the signal is expected to be proportional to the pulse duration. Normalization of both spectra to the N₂⁺ ion peak, which is also saturated, gives the observed equivalent heights.

In conclusion, molecular multiple ionization occurs at short internuclear distances close to the neutral molecule equilibrium distance using ultrashort 10-fs laser pulses. The main consequences are higher Coulomb explosion kinetic energy releases and lower fragmentation yields. This work opens the route to Coulomb explosion imaging of neutral

molecular species using small-scale laser-based experiments.

The authors are pleased to acknowledge M. Bougeard and E. Caprin for their skilled technical assistance, the support of INTAS Grant No. 99-01495, and the support of ACI Photonique Physique Attoseconde.

-
- [1] Z. Vager, R. Naaman, and E. Kanter, *Science* **244**, 426 (1989).
[2] L. Frasinski, K. Codling, P. Hatherly, J. Barr, I. Ross, and W. Toner, *Phys. Rev. Lett.* **58**, 2424 (1987).
[3] C. Cornaggia, J. Lavancier, D. Normand, J. Morellec, P. Agostini, J.-P. Chambaret, and A. Antonetti, *Phys. Rev. A* **44**, 4499 (1991).
[4] *Molecules and Clusters in Intense Laser Fields*, edited by J. Posthumus (Cambridge University Press, 2001).
[5] S. Chelkowski and A. Bandrauk, *J. Phys. B* **28**, L723 (1995).
[6] P. Maine, D. Strickland, P. Bado, M. Pessot, and G. Mourou, *IEEE J. Quantum Electron.* **24**, 398 (1988).
[7] V. Bagnoud and F. Salin, *Appl. Phys. B: Lasers Opt.* **70**, S165 (2000).
[8] S. Sartania, Z. Cheng, M. Lenzner, G. Tempea, C. Spielmann, F. Krausz, and K. Ferencz, *Opt. Lett.* **22**, 1562 (1997).
[9] M. Nisoli, S. D. Silvestri, and O. Svelto, *Appl. Phys. Lett.* **68**, 2793 (1996).
[10] R. Szipöcs, K. Ferencz, C. Spielmann, and F. Krausz, *Opt. Lett.* **19**, 201 (1994).
[11] W. Wiley and I. McLaren, *Rev. Sci. Instrum.* **26**, 1150 (1955).
[12] L. Frasinski, K. Codling, and P. Hatherly, *Science* **246**, 973 (1989).
[13] C. Cornaggia and P. Hering, *Phys. Rev. A* **62**, 023403 (2000).
[14] C. Beylerian and C. Cornaggia, *J. Phys. B* **37**, L259 (2004).
[15] A. Bandrauk, D. Musaev, and K. Morokuma, *Phys. Rev. A* **59**, 4309 (1999).
[16] M. Besnard, L. Hellner, G. Dujardin, and D. Winkoun, *J. Chem. Phys.* **88**, 1732 (1988).
[17] J. Senekowitsch, S. O'Neil, and W. Meyer, *Theor. Chim. Acta* **84**, 85 (1992).
[18] A. Remscheid, B. Huber, M. Pykavyj, V. Staemmler, and K. Wiesemann, *J. Phys. B* **29**, 515 (1996).